

This document is accepted manuscript for publication in Advances in Space Research.

Published version of this manuscript is found at <https://doi.org/10.1016/j.asr.2015.06.037>

This work is licensed under the Creative Commons Attribution-NonCommercial-NoDerivatives 4.0 International License. To view a copy of this license, visit <http://creativecommons.org/licenses/by-nc-nd/4.0/> or send a letter to Creative Commons, PO Box 1866, Mountain View, CA 94042, USA.

1 **Detectability of hydrous minerals using ONC-T camera onboard the**
2 **Hayabusa-2 spacecraft**

3

4 S. Kameda^a, H. Suzuki^b, Y. Cho^a, S. Koga^c, M. Yamada^d, T. Nakamura^e, T.
5 Hiroi^f, H. Sawada^g, R. Honda^h, T. Morotaⁱ, C. Honda^j, A. Takei^a, T.
6 Takamatsu^a, Y. Okumura^a, M. Sato^a, T. Yasuda^a, K. Shibasaki^a, S. Ikezawa^a,
7 S. Sugita^c

8

9 ^a Department of Physics, Rikkyo University, 3-34-1 Nishi-Ikebukuro, Toshima, Tokyo
10 171-8501, Japan

11 ^b Department of Physics, Meiji University, 1-1-1, Higashi-Mita, Tama-ku, Kawasaki,
12 Kanagawa 214-8571, Japan

13 ^c Department of Earth and Planetary Science, Graduate School of Science, University of
14 Tokyo, 7-3-1 Hongo, Bunkyo-ku, Tokyo 113-0033, Japan

15 ^d Planetary Exploration Research Center, Chiba Institute of Technology, 2-17-1 Tsudanuma,
16 Narashino, Chiba 275-0016, Japan

17 ^e Division of Earth and Planetary Materials Science, Graduate School of Science, Tohoku
18 University, Aoba, Sendai, Miyagi 980-8578, Japan

19 ^f Department of Earth, Environmental and Planetary Sciences, Brown University,
20 Providence, Rhode Island 02912, USA

21 ^g Japan Aerospace Exploration Agency, JAXA Space Exploration Center, HAYABUSA2
22 Project, 3-1-1 Yoshinodai, Chuo-ku, Sagami-hara, Kanagawa 252-5210, Japan

23 ^h Natural Sciences Cluster-Science Unit, Kochi University, 2-5-1 Akebono-cho, Kochi,
24 Kochi 780-8520, Japan

25 ⁱ Graduate School of Environmental studies, Nagoya University, Furo-cho, Chikusa, Nagoya,
26 Aichi 464-8601, Japan

27 ^j Research Center for Advanced Information Science and Technology, The University of Aizu,
28 Tsuruga, Ikkimachi, Aizuwakamatsu, Fukushima 965-8580, Japan

29

30

31

32

33 Corresponding Author: Shingo Kameda (kameda@rikkyo.ac.jp)

34 **Abstract**

35 The Hayabusa-2 spacecraft has three framing cameras (ONC-T, ONC-W1,
36 and ONC-W2) for optical navigation to asteroid 1999 JU₃. The ONC-T is a
37 telescopic camera with seven band-pass filters in the visible and
38 near-infrared range. These filters are placed on a wheel, which rotates to put
39 a selected filter for different observations, enabling multiband imaging.
40 Previous ground-based observations suggesting that hydrous materials may
41 be present on the surface of 1999 JU₃ and distributed in relatively limited
42 areas. The presence of hydrous minerals indicates that this asteroid
43 experienced only low to moderate temperatures during its formation,
44 suggesting that primordial materials are preserved. In order to find the best
45 sampling sites, we will perform reflectance spectroscopic observations using
46 the ONC-T near the asteroid after arrival. Finding regions rich in hydrous
47 minerals is the key for this remote sensing observation. In preparation for
48 this, we conducted ground-based experiments for the actual ONC-T flight
49 model to confirm the detectability of the absorption band of Fe-rich
50 serpentine. As a result, we detected the absorption band near 0.7 μm by
51 reflectance spectroscopy of CM2 chondrites, such as Murchison and Nogoya,
52 which are known to contain the Fe-rich serpentine, and did not detect any
53 0.7 μm absorption in Jbilet Winselwan CM2 chondrite with decomposed
54 Fe-rich serpentine.

55

56 **1. Introduction**

57 Hayabusa-2 is a sample-return mission to the asteroid 162173 1999 JU₃
58 (Tsuda et al., 2013, Ishiguro et al., 2014). The spacecraft was launched on
59 December 3, 2014, and is expected to arrive at the asteroid in 2018, and
60 return to Earth in 2020. Asteroid 1999 JU₃ is one of the near-Earth C-type
61 asteroids (Binzel et al., 2001, Campins et al., 2013). Vilas (2008) found that
62 the reflectance spectrum has an absorption feature centered near 0.7 μm,
63 which indicates the presence of iron-bearing phyllosilicates and primordial
64 or aqueously altered early solar system material on the surface of the
65 asteroid. The objective of the Hayabusa-2 mission is to return samples from
66 1999 JU₃. On the other hand, only the July 2007 spectrum has a 0.7 μm

67 absorption feature, and the other reflectance spectra in the visible and
68 near-infrared range obtained by the ground-based observations do not show
69 a clear 0.7 μm feature (Moscovitz et al. (2013), Lazzaro et al. (2013), and
70 Sugita et al. (2013)). The signal to noise ratio (S/N) of their observation may
71 not high enough for detection of a 3–4% absorption near 0.7 μm , which is
72 typical for Murchison and Murray CM2 chondrites including iron-bearing
73 phyllosilicates (Cloutis et al., 2011). If any hydrous minerals with 0.7 μm
74 absorption are present, they may be distributed only in relatively limited
75 areas and/or during a limited time period.

76 To locate hydrous minerals, Hayabusa-2 has a multi-band imager. The
77 optical navigation camera (ONC) system onboard the Hayabusa-2 spacecraft
78 consists of one telescopic camera (T) and two wide-angle cameras (W1 and
79 W2). These cameras are similar to those installed on the Hayabusa
80 spacecraft (Ishiguro et al., 2010). Table 1 shows the specifications of ONC-T
81 and figure 1 shows the transmittance spectra of the band-pass filters. The
82 ONC-T has a wheel with seven band-pass filters and one panchromatic glass
83 window for correction of the light path length. The center wavelengths of the
84 filters are 0.39 μm (ul-band), 0.48 μm (b-band), 0.55 μm (v-band), 0.59 μm
85 (Na), 0.70 μm (x-band), 0.86 μm (w-band), and 0.95 μm (p-band). These filters
86 were selected based on the filters on the Hayabusa spacecraft. In the design
87 phase of ONC for the Hayabusa mission, the filters were selected based on
88 the 8 filters used by the Eight Color Asteroid Survey (ECAS) (Zellner et al.,
89 1985). The names of the filters except for 0.59 μm (Na) are the same in 6
90 cases as the ECAS filters. The zs-band filter (1.05 μm) used in Hayabusa was
91 changed to Na filter for Hayabusa-2, and the center wavelength and
92 bandwidth of b-band filter was slightly changed.

93 During the time between arriving at 1999 JU₃ and the first touchdown,
94 the Hayabusa-2 spacecraft will stay at the home position (HP) altitude of 20
95 km and obtain the global multi-band spectral image, which is useful for
96 determination of the first touchdown point. Vilas (1994) detected a 0.7 μm
97 absorption feature in the ground-based observations of C-class asteroids
98 using the ECAS filters. In order to demonstrate the ability of the
99 spectroscopic mapping observations in a laboratory before launch, we

100 performed multi-band spectral imaging of CM2 chondrites (Murchison,
101 Nogoya, and Jbilet Winselwan) using the ONC-T flight model and examined
102 its detectability of hydrous minerals.

103

104 **2. Experiment**

105 The absorption of hydrous minerals near $0.7\ \mu\text{m}$ is only $\sim 3\%$, and its full
106 width of half maximum is $\sim 0.1\ \mu\text{m}$ (Cloutis et al., 2011). ONC-T has filters
107 centered at $0.55\ \mu\text{m}$, $0.70\ \mu\text{m}$, and $0.86\ \mu\text{m}$. To detect the absorption at 3% ,
108 S/N for each band should be higher than ~ 122 . ONC-T has a $1\ \text{K} \times 1\ \text{K}$ -pixel
109 ($13\text{-}\mu\text{m}$ square pixel) CCD with a 12-bit analog-to-digital converter. One
110 analog-to-digital unit (ADU) corresponds to 21 electrons. We set the exposure
111 time so that the intensity of the light is more than 2000 ADU, which
112 corresponds to $\sim 42,000\ \text{e}$, and the S/N is more than 200. The exposure times
113 were 2.8 s (ul), 131 ms (b), 87 ms (v), 131 ms (Na), 33 ms (w), 87 ms (x), and
114 348 ms (p). The electrical random noise generated by the detector and the
115 electronics in readout is negligible ($\sim 2\ \text{ADU}$). The dark noise is smaller than
116 $\sim 50\ \text{ADU}$ in ul-band and $\sim 5\ \text{ADU}$ in other bands in the room temperature
117 during the exposure time. After dark noise correction, the random noise
118 caused by the dark current is reduced to $\sim 1.5\ \text{ADU}$. Therefore, the photon
119 noise is dominant in this experiment. The bias offset can be subtracted using
120 the blind region of CCD pixels.

121 To examine the detectability of the absorption near $0.7\ \mu\text{m}$, we used CM2
122 chondrites: Murchison (pellet), Nogoya (chip), and Jbilet Winselwan (slab).
123 Figure 2a shows the configuration of our experiment. Because the depth of
124 field of ONC-T is more than 100 m, we set an achromatic lens with a focal
125 distance of 150 mm in front of ONC-T. The focal length of ONC-T is 120 mm;
126 consequently, the magnification ratio is 1.25. The angular resolution is 0.1
127 mili-radian. Without the achromatic lens, the spatial pixel resolution at the
128 asteroid surface is 2 m/pix when the spacecraft is at the HP altitude (20 km).
129 The phase angle of the light-source sample camera was set at 30 degrees.

130 We performed the experiment inside a dark room installed in a clean
131 room at JAXA. The stray light was carefully reduced because the reflectance
132 of the samples is low ($\sim 5\%$). We used an adjustable aperture in front of the

133 light source to illuminate only the sample surface and covered all the parts
134 near the light path with black flock paper (Figure 2b). We used a halogen
135 lamp (LA-100USW) without a thermal filter as a light source. The stability of
136 the output was confirmed to be less than required (0.3%) during the
137 experiment.

138 We obtained seven-band images of each sample and used a standard
139 reflective plate to estimate the reflectance of the sample. A white standard
140 reflector called Spectralon (Labsphere SRS-99-20; $R \sim 100\%$) is commonly
141 used for reflectance measurements. The absorption depth of 3% is relative to
142 the reflectance averaged from 0.55 μm to 0.86 μm . The average reflectance is
143 $\sim 5\%$ for 1999 JU₃ and CM2 chondrites, therefore, the absolute absorption
144 depth with respect to the incident flux is very small (0.15%). To reduce the
145 requirement for dynamic range of our experiment, we used a black standard
146 reflector (SRS-05-020) for a reference, the reflectance of which was measured
147 as $\sim 5\%$ in the visible and near-infrared ranges.

148

149 3. Results

150 Figure 3a shows an image of a Murchison chondrite obtained with the
151 v-band filter. The roughness of the sample surface is clearly seen in the
152 obtained images because the spatial resolution at the sample surface is ~ 16
153 μm and the grain size is $\sim 100 \mu\text{m}$. Figure 3b shows the reflectance spectra
154 normalized at the wavelength of 550 nm, averaged in 70×70 pixels. The
155 absorption depth (d_a) is calculated from the v-, w-, and x-band reflectances
156 (R_v , R_w , and R_x) as given by the following equation:

$$157 \quad d_a = 1 - \frac{3.1 R_w}{1.6 R_v + 1.5 R_x} . \quad (1)$$

158 The coefficients are determined by taking into account the difference of
159 the center wavelengths of the v-, w-, and x-band filters (0.55 μm , 0.70 μm ,
160 and 0.86 μm). In the case that the spectrum is linear between v-band and
161 x-band, d_a equals to zero.

162 For the Murchison chondrite (pellet), the absorption depth was measured
163 as $\sim 3\%$. We selected three regions without any hot pixels or glare due to
164 specular reflection on grain surfaces. The reflectance spectra of the three

165 regions conform to one another, although the reflectance at 0.86 μm and 0.95
166 μm is slightly variable. In the three regions shown in Figure 3a, the average
167 absorption depth is 2.9%, and the maximum deviation from the average is
168 0.3%. This suggests that the 0.7 μm absorption band caused by hydrous
169 minerals can be detected by ONC-T.

170 Figure 4a shows an image of a part of the Nogoya chondrite (chip) with
171 the v-band filter. We can see a bright chondrule near the center of the field of
172 view. We selected three regions again (Figure 4a). Two are for the matrix,
173 and one is for the chondrule. Figure 4b shows the reflectance spectra
174 normalized at the wavelength of 0.55 μm , averaged in 50×50 pixels. The
175 absorption depth of the matrix is 3.8% (Figure 4 A) and 4.2% (Figure 4 B)
176 and that of the chondrule is 0.0% (Figure 4 C). This result suggests that the
177 matrix contains hydrous minerals and that a chondrule does not contain a
178 detectable amount of Fe-rich serpentine.

179 An image of a part of the Jbilet Winselwan chondrite (slab) with the
180 v-band filter is shown in Figure 5a. Figure 5b shows that the absorption
181 depth is below zero in the three regions, which suggests that this chondrite
182 does not contain crystalline Fe-rich serpentine, consistent with a previous
183 mineralogical and optical study of this chondrite (Nakamura et al., 2014).

184 The estimation of the systematic error is difficult. However, it is also
185 difficult to explain that systematic differences in the measurements cause
186 the detection of absorption in Murchison and Nogoya and no absorption in
187 Jbilet Winselwan. We concluded that the ONC-T can detect the 0.7 μm
188 absorption band caused by hydrous minerals and some additional in-flight
189 and ground-based measurements are necessary for qualitative evaluation.

190

191 **4. Summary and future work**

192 We performed experiments using the ONC-T instrument to demonstrate
193 its ability to detect and locate the hydrous minerals on the asteroid 1999 JU₃.
194 The three CM2 chondrites are used, Murchison (pellet), Nogoya (chip), and
195 Jbilet Winselwan (slab). As a result, the absorption of hydrous minerals
196 centered near 0.7 μm was detected for Murchison and Nogoya, which contain
197 Fe-rich serpentine, and was not detected for Jbilet Winselwan with

198 decomposed Fe-rich serpentine.

199 For observation of the asteroid, we must take into account the spin of the
200 asteroid. The exposure time is 0.1—0.3 s and it takes approximately 5
201 seconds for rotation of the filter wheel to change bandpass filters. The field of
202 view at the asteroid surface significantly changes during this operation. To
203 obtain the correct reflectance spectrum, we have to coregister the position of
204 the field of view of the images of different bands. The sensitivity instability
205 due to the temperature change will be small because the total time for
206 7-color imaging is short (~100 s). We should conduct experiments to evaluate
207 and compensate for the systematic error caused by this imperfect
208 coregistration, taking into account the flat field correction imperfection. For
209 in-flight calibration, instead of a black reference, we should use the standard
210 solar spectrum (e.g., ASTM E-490) and sensitivity calibration data via
211 in-flight standard star observation and pre-flight flat field measurements
212 using an integration sphere. Though the degradation of the lens in space is
213 estimated to be low, the standard star observation should be performed just
214 before and after the asteroid observation, or frequently enough to confirm
215 that the degradation is negligible.

216 Additionally, the phase angle was fixed to be 30 degrees in our
217 experiment. However, the actual phase angle for Hayabusa-2 varies from 0
218 to 40 degrees. We are planning an additional reflectance spectroscopy
219 experiment with the various phase angles using the laboratory test model of
220 ONC-T.

221

222

223 **Acknowledgement**

224 The authors wish to thank Dr. S. Nakazawa, Dr. Y. Tsuda, Dr. K. Ogawa, and
225 Hayabusa-2 team for supporting our experiment and managing the schedule
226 of the very rushing project. The authors also wish to thank Dr. Y. Iijima for
227 supporting our activities.

228

229 **References**

230 Binzel, R.P., Harris, A.W., Bus, S.J., and Burbine, T.H., Spectral properties of

231 near-Earth objects: Palomar and IRTF results for 48 objects including
232 spacecraft targets (9969) Braille and (10302) 1989 ML. *Icarus* 151, 139–149,
233 2001, doi:10.1006/icar.2001.6613
234
235 Campins, H., de León, J, Morbidelli, A., et al., The Origin of Asteroid 162173
236 (1999 JU₃), *AJ* 146, 26, 2013, doi:10.1088/0004-6256/146/2/26
237
238 Cloutis, E. A., Hudon, P., Hiroi, T., et al., Spectral reflectance properties of
239 carbonaceous chondrites: 2. CM chondrites, *Icarus* 216, 309, 2011,
240 doi:10.1016/j.icarus.2011.09.009.
241
242 Ishiguro, M., Nakamura, R., Tholen, D. J., et al., The Hayabusa Spacecraft
243 Asteroid Multi-band Imaging Camera (AMICA), *Icarus* 207, 714, 2010,
244 doi:10.1016/j.icarus.2009.12.035
245
246 Ishiguro, M., Kuroda, D., Hasegawa, S., et al., Optical Properties of (162173)
247 1999 JU₃: In preparation for the JAXA Hayabusa 2 Sample Return Mission,
248 2014, *ApJ* 792, 74, 2014, doi:10.1088/0004-637X/792/1/74
249
250 Lazzaro, D., Barucci, M. A., Perna, D., et al., Rotational spectra of (162173)
251 1999JU₃, the target of the Hayabusa2 mission, *A&A* 549, L2, 1, 2013, doi:
252 10.1051/0004-6361/201220629
253
254 Moskovitz, N. A., Abe, S., Pan, K.-S., et al., Rotational characterization of
255 Hayabusa II target Asteroid (162173) 1999 JU₃, 2013, *Icarus*, 224, 24, doi:
256 10.1016/j.icarus.2013.02.009
257
258 Nakamura, T., Iwata, T., Kitasato, K., et al., Reflectance spectra
259 measurement of hydrated and dehydrated carbonaceous chondrites using
260 the Near Infrared Spectrometer on Hayabusa 2 spacecraft, *Antarctic*
261 *Meteorites XXXVII*, 54, 2014.
262
263 Sugita, S., Kuroda, D., Kameda, S., et al., Visible Spectroscopic Observations

264 of Asteroid 162173 (1999 JU₃) with the Gemini-S Telescope, LPI
265 Contributions, 1719, 2591, 2013
266
267 Tsuda, Y., Yoshikawa, M., Abe, M., et al., System design of the Hayabusa
268 2—Asteroid sample return mission to 1999 JU₃, Acta Astronautica 91, 356,
269 2013, doi:10.1016/j.actaastro.2013.06.028
270
271 Vilas, F., A Cheaper, Faster, Better Way to Detect Water of Hydration on
272 Solar System Bodies, Icarus 111, 456, 1994
273
274 Vilas, F., Spectral characteristics of Hayabusa 2 Near-Earth Asteroid targets
275 162173 1999 JU₃ and 2001 QC₃₄, AJ 135, 1101, 2008, doi: 10.1088/
276 0004-6256/135/4/1101
277
278 Zellner, F., Tholen, D. J., and Tedesco, E. F., The Eight-Color Asteroid
279 Survey: Results for 589 Minor Planets, Icarus 61, 1355, 1985
280
281

282 Figure 1: The transmittance spectra of the band-pass filter installed on the
283 wheel in ONC-T. ONC-T has 7 filters (ul, b, v, Na, w, x, p) and a
284 panchromatic glass window. The center wavelengths of the filters are 390 nm,
285 480 nm, 550 nm, 589 nm, 700 nm, 860 nm, and 950 nm, respectively. The
286 accuracy of the transmittance is less than 1%.

287

288 Figure 2: (a) Schematic diagram for the experimental configuration . An
289 achromatic lens with a focal distance of 150 mm was set in front of ONC-T.
290 The phase angle of the light-source sample camera was set at 30 degrees. (b)
291 Inside the black room. The parts near the light path were covered with black
292 flock paper (arrows).

293

294 Figure 3: (a) A v-band image of Murchison (pellet). (b) The multi-band
295 spectra of the three region shown in (a). Spectra are scaled to 1.0 at 550 nm.

296

297 Figure 4: (a) A v-band image of Nogoya (chip). (b) The multi-band spectra of
298 the three region shown in (a). Spectra are offset by a reflectance of 0.2 for
299 clarity.

300 Figure 5: (a) A v-band image of Jbilet Winselwan (slab). (b) The multi-band
301 spectra of the three region shown in (a).

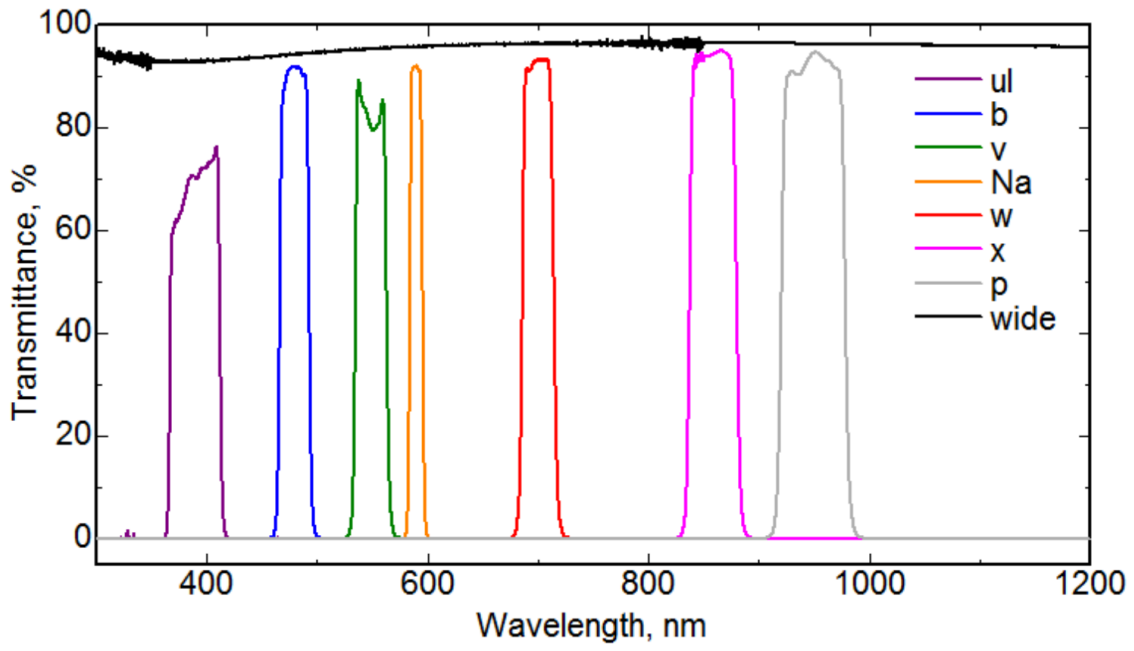
302 **Table 1: ONC-T specification**

Optics	Focal Length	120mm
	F#	8
	Effective aperture	φ15 mm
	Field of View	6.35 deg × 6.35 deg
	Pixel resolution	22 arcsec/pixel
	Depth of field	100 m ~ infinity
	Transmittance of ND filter	30%
Filter Wheel	Band pass filter	#1 : ul 0.39 μm , #2 : Wide*, #3 : v 0.55 μm, #4 : w 0.70 μm, #5 : x 0.86 μm, #6 : Na 0.59 μm, #7 : p 0.95 μm, #8 : b 0.48 μm
	Filter wheel driving rate	9.6 deg/sec (4.69sec/Filter)
CCD	CCD	e2v CCD47-20 (AIMO)
	Pixel format	1024(H) pixel×1024(V) pixel
	Pixel pitch	13 μm × 13 μm
Electronics	Dynamic range	10 bit
	A/D bit length	12 bit

303 **Wide** is a panchromatic glass window for light path length correction

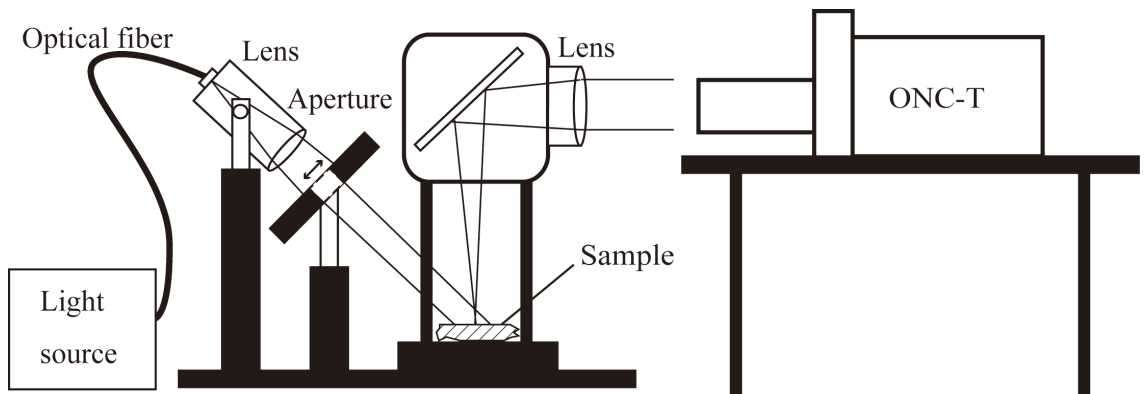
304

305



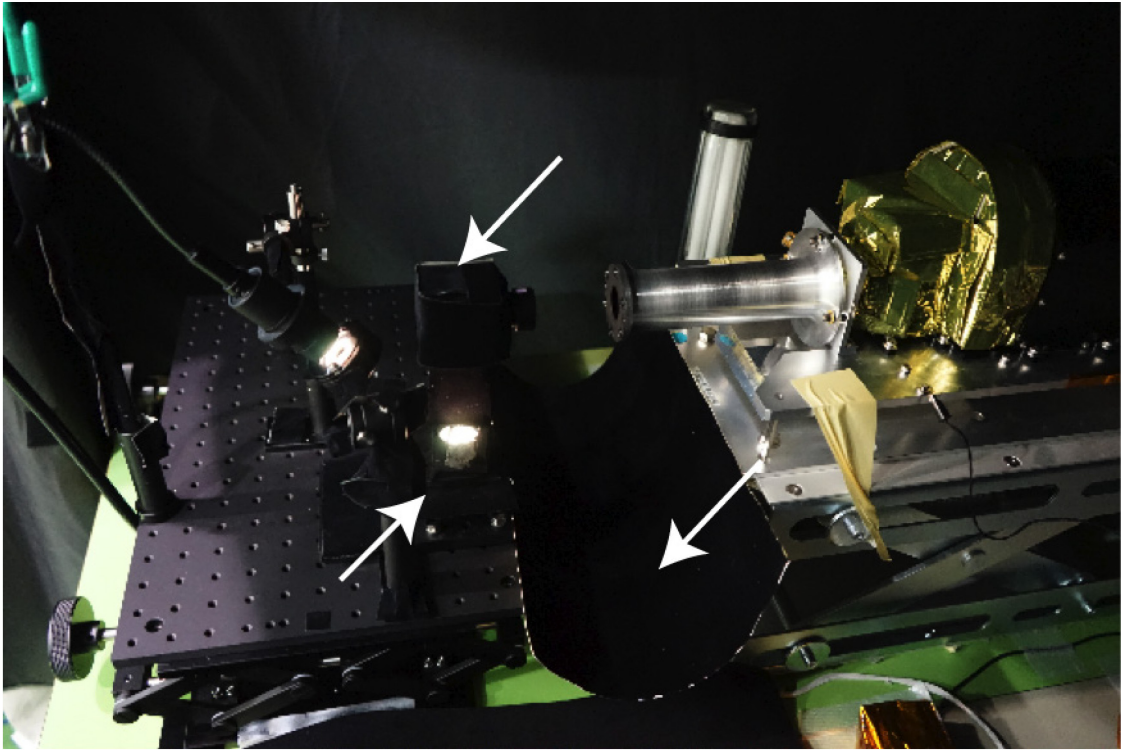
306

307 Fig. 1



308

309 Fig. 2a



310

311 Fig. 2b

312

313

314

315

316

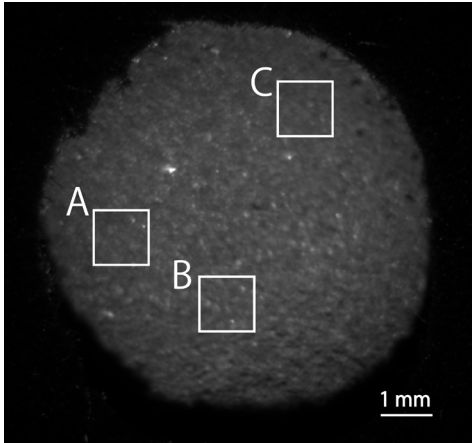


Fig. 3a

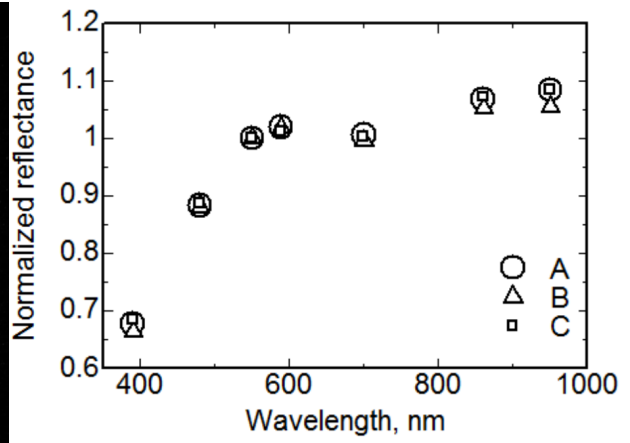


Fig. 3b

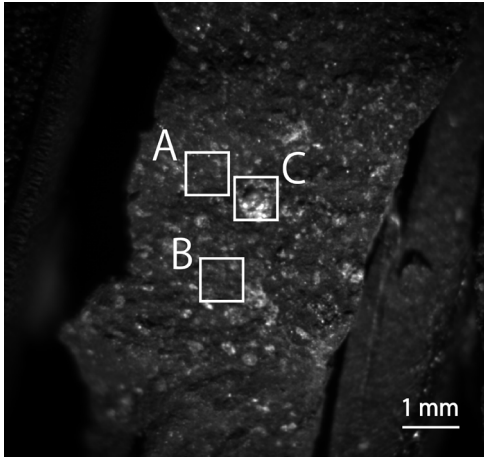


Fig. 4a

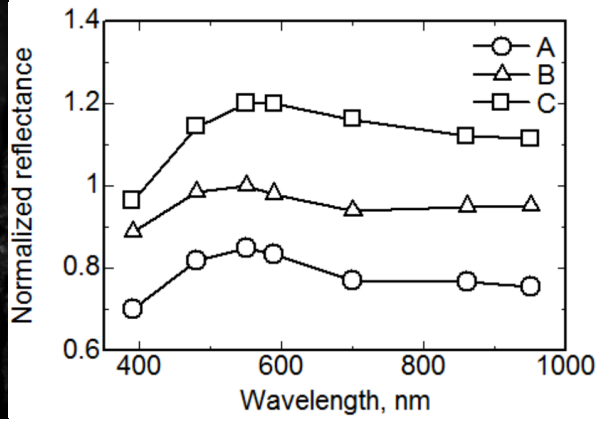


Fig. 4b

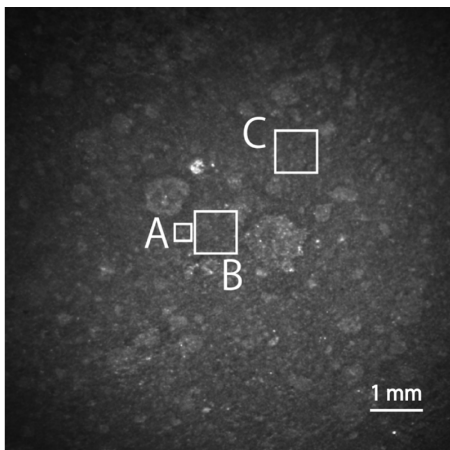


Fig. 5a

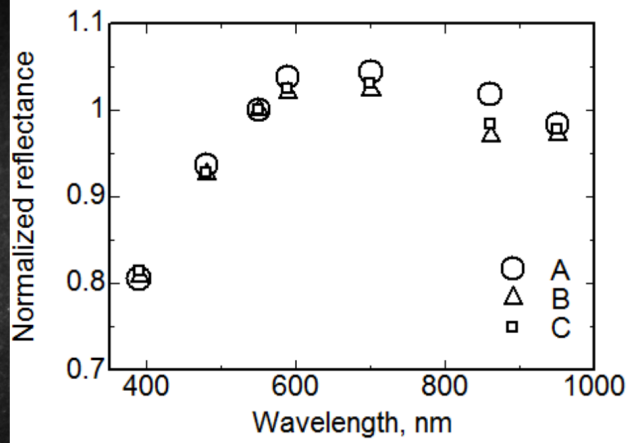


Fig. 5b

317

318

319

320

321

322

323

324

325